IEEE Access
Multidisciplinary | Rapid Review | Open Access Journal

Received 24 August 2022, accepted 7 September 2022, date of publication 12 September 2022,
date of current version 22 September 2022.

Digital Object Identifier 10.1109/ACCESS.2022.3206363

RESEARCH ARTICLE

Automatic Hajj and Umrah Ritual Detection Using IMU Sensors

KHALIL CHIKHAOUI[1], MOHAMMED ELRASHIDY[1], MOTAZ ALFARRAJ[1,2], (Member, IEEE), ALI H. MUQAIBEL[1,3], (Senior Member, IEEE), RIDA SADAGAH[1], AND ABDULLAH SHARQAWI[1]

[1]Electrical Engineering Department, King Fahd University of Petroleum and Minerals, Dhahran 31261, Saudi Arabia
[2]SDAIA-KFUPM Joint Research Center for Artificial Intelligence, King Fahd University of Petroleum and Minerals, Dhahran 31261, Saudi Arabia
[3]Center for Communication Systems and Sensing, King Fahd University of Petroleum and Minerals, Dhahran 31261, Saudi Arabia

Corresponding author: Motaz Alfarraj (motaz@kfupm.edu.sa)

The authors would like to acknowledge the Deanship of Research Oversight and Coordination (DROC) at King Fahd University of Petroleum & Minerals (KFUPM) for the support under SDAIA-KFUPM Joint Research Center for Artificial Intelligence and the Interdisciplinary Research Center for Communication Systems and Sensing

ABSTRACT A smartphone can provide a wide range of practical applications and services thanks to its advanced sensing capabilities. However, the sector of Hajj and Umrah, which are rituals performed by millions of pilgrims, still lacks intelligent solutions that can improve the pilgrim experience using these sophisticated capabilities. This research aims to bridge this gap by introducing a solution that applies a real-time monitoring process to different Umrah activities (i.e., Tawaf and Sa'i) using smartphone sensors. In the proposed solution, the smartphone first tracks the pilgrim's path with the help of inertial sensors, commonly known as the inertial measurement unit (IMU). Then, an algorithm is developed to detect and process the different activities performed by the user and provide helpful instructions accordingly for a comfortable and successful experience. The proposed system was tested and validated using real data for Tawaf and Sa'i activities. The extracted paths were compared with the GPS data for validation. Results showed that the paths were extracted effectively and the algorithm monitored both Tawaf and Sa'i successfully. The deviation between the real path and the extracted path using the proposed algorithm can be enhanced with proper GPS assessment and step-length calibration.

INDEX TERMS Activity detection, Hajj, IMU sensing, indoor navigation, path tracking, PDR, Umrah.

I. INTRODUCTION

Tawaf, walking seven laps around the Kaaba while reciting supplications and prayers, and Sa'i, walking between Safa and Marwa seven times while reciting supplications and prayers, are important rituals performed by millions of Muslims throughout the year. The combination of the two of them is known to Muslims as Umrah. Tawaf and Sa'i are also part of the annual Islamic pilgrimage known as Hajj. According to the Saudi General Authority of Statistics [1], the total number of Muslims who performed Umrah in 2019 reached 19 million. Also, with up to 3 million pilgrimages gathered between the 8th and the 13th of Dhu al-Hijjah, the twelfth month in the Islamic calendar, Hajj is the largest annual mass gathering globally [2]. The gathering of such huge numbers normally creates big crowds that must be carefully managed to provide a smooth experience.

The associate editor coordinating the review of this manuscript and approving it for publication was Shaohua Wan.

The potential of smartphones remains untapped in the sector of Hajj and Umrah. In a study published in Khan and Shambour [3] investigated more than 200 applications used to help pilgrims in the holy rituals. Results indicated that most of these applications are primitive and provide very basic services to the user. Examples of these services included information on Hajj and Umrah rituals, live video, Qibla (i.e., the direction towards which Muslim people face during prayers) compass, and prayer schedule. We aim in this work to bridge this gap by providing a smart solution that can be used to benefit Hajj and Umrah sector. Namely, we design a real-time, interactive, and automated Umrah detection service that utilizes smartphone sensors. A smartphone application collects the data from the smartphone's motion sensors. Then, an algorithm is designed to deliver useful information to the pilgrim upon automatic identification and processing of their Umrah activities. The delivered information includes lap count, interactive guidance, supplications, and general statistics about Umrah.

The proposed system is expected to help in managing the crowds and reduce the congestion in Hajj and Umrah through autonomous detection and interactive guidance. Also, this work can be extended to control and monitor other mass gatherings such as large festivals and religious pilgrimages.

A. RELATED WORK

Human activity recognition has gained increasing attention for the past three decades [4], [5], [6], [7]. Different activity recognition techniques are implemented using motion sensors (e.g., accelerometers [8], [9], [10]), microphones [11], [12], and cameras [13] to infer different sets of human activities. The settings of different activity detection techniques fall into two categories. In the first category, the employed sensors are embedded in a wearable device [10], [14]. The second category includes systems that use smartphone-embedded sensors for activity recognition [15], [16]. Wearable sensors have the advantage of providing a controlled relationship between the sensor data and the target activity. However, in the second category, more sophisticated algorithms are required to predict this relation. Nonetheless, it is more feasible and cost-efficient to use smartphone sensors for large target population events such as Hajj and Umrah.

Different approaches for activity recognition from both categories target activities like walking, running, cycling, sleeping, and making conversations. However, a pilgrim performs a collection of these activities during any of the Umrah rituals. Since the main objective of this work is to detect these rituals (i.e., Tawaf and Sa'i), utilizing simple activity recognition techniques will not be sufficient for detecting more complex activities like the ones performed during Umrah. Therefore, we attempt a different approach where pilgrim's ritual activities can be inferred from tracking and analyzing their walking path. Existing smartphone applications used for similar tasks (e.g., Tawaf App [17] and Al-Maqsad [18]) use hybrid approaches for path tracking based on Bluetooth Low Energy (BLE), Wi-Fi, and GPS. For utilizing such resources, external tag installation is required. Moreover, direct user interaction is required for the mentioned applications to be able to recognize the starting point of the ritual. Finally, each application specializes in detecting a specific activity (e.g., counting the number of laps during Tawaf or indoor navigation). However, none of these applications are designed for detecting all Umrah activities.

Different techniques employ smartphone sensors for positioning purposes. Ashraf *et al.* [19] reviewed such techniques, including Wi-Fi, BLE, Pedestrian Dead Reckoning (PDR), Geomagnetic, GPS, and camera-based localization. Except for PDR, though, other techniques require either external infrastructure [20], which is not available in Tawaf and Sa'i areas, or relatively high power consumption [19], [21]. Indoor localization techniques generally suffer from the first drawback, since they are mostly designed to leverage Wi-Fi tags (e.g., [22]). Yu *et al.* [20] attribute the mentioned issues to navigation methods other than inertial navigation, which includes strapdown inertial navigation systems (SINS) and PDR. SINS is specifically used when the IMU unit is rigidly attached to the tracked object [23] or, in the case of pedestrian tracking, mounted to the user's feet [20]. PDR, on the other hand, does not suffer from this limitation [20]. Considering its capability of tracking pedestrians using IMU units embedded in smartphones, we choose PDR for path tracking.

PDR technique [24], [25], [26], [27] used for path tracking in this work consists of two main stages. The first stage is step counting and travel distance estimation. The second stage is heading estimation. Algorithms that use smartphone sensor data to achieve the objectives of each stage can be found either separately or combined in the literature. Step counting is a topic of interest for many researchers. Brajdic and Harle [28] evaluated different step counting and walk detection algorithms at six different phone positions. The authors reported that windowed peak detection methods for accelerometer data are favored for step detection with an error rate of less than 3%. A more recent work [29] proposed an algorithm that defines three measures for analyzing the accelerometer data: periodicity, similarity, and continuity. A step is verified when these three measures meet certain conditions. The algorithm outperformed the conventional peak detection-based method. Relying on measures such as similarity and periodicity may require the studied walk to be uniform to a certain degree. During Umrah, though, pilgrims' movements are expected to be more complex considering the usual crowd situations in Tawaf and Sai areas. Rodríguez *et al.* [30] presented a model where peak-valley detection is used for step counting. They used a combination of support vector machines and a standard deviation-based classifier for validating the results of the standard step counting strategy. Pham *et al.* [31] proposed an algorithm that finds suitable minimal peak detection, minimal peak prominence, dynamic thresholding, and vibration elimination and leverages them to solve problems like over-counting, under-counting, and false walking which can be encountered by the standard method. The methodology was tested on a peak detection algorithm. It is also common to use fast Fourier transform (FFT) to detect and count steps [32], [33].

Works focusing on heading estimation usually propose a mathematical model that fuses the fetched data from IMU units to determine the device's 3D orientation via either Euler's angles or quaternions. The fusion process usually involves Kalman filters, and sometimes quaternions. The next step is to use the orientation of the device along with the data from the IMU unit to estimate the heading of the user [34], [35], [36]. It is important to notice, though, that smartphones readily provide the pitch, roll, and azimuth of the device using a virtual sensor called *the orientation sensor*. This sensor is created using a fusion process similar to the one described above [37].

B. CONTRIBUTION

While the above mentioned works utilize step counting and heading estimation techniques to detect relatively simple

actions like walking and running, the main contribution of this work is to use the path found by applying PDR to recognize more complicated actions, namely, Tawaf and Sa'i. In this work, we design a system that is implemented on a mobile application.[1] In summary, this system is composed of two steps that enable ritual detection in real-time. The two steps are:

- Developing a PDR algorithm for path tracking. The algorithm is customized for the Umrah rituals and provides reliable tracking in indoor and outdoor environments using the smartphone sensors only without any external infrastructure needed.
- Developing an algorithm to detect and monitor Tawaf and Sa'i activities automatically without user activation (The application will collect GPS data periodically in the background "upon user approval" and the detection process automatically starts when the user is within the Tawaf area).

Since the objective of this work is to detect Umrah rituals given the pilgrim's path, the developed PDR technique is similar to what can be found in the literature. For step counting, a peak detection method is followed after fetching and filtering the accelerometer data. A similar approach can be found in [38]. For heading estimation, the output of the orientation sensor will be directly used, along with accelerometer correction. The role of PDR in this paper is to provide a path that can be appreciated by the detection algorithm. Therefore, aiming for a robust, novel, PDR algorithm is not one of the objectives of this work.

Finally, this work is expected to contribute to important aspects related to organization tasks in Masjid al-Haram like crowd management in Tawaf and Sa'i areas.

The rest of the paper is organized as follows. Section II introduces the system framework and explains the underlying processes that include pre-processing of sensors' readings (Section II-A), path tracking using PDR (Section II-B), and real-time detection and monitoring (Section II-C). Section III provides results analysis for the different stages in the proposed model. Finally, the paper is concluded in Section V.

II. SYSTEM FRAMEWORK

We propose a 3-stage system as shown in Fig. 1. The inputs to the system come from three sensors in the user's smartphone; accelerometer, orientation sensor, and GPS. The readings of the accelerometer and the orientation sensor are provided by the inertial measurement unit (IMU) in the smartphone. The data is passed sequentially through the three stages of the system.

In the first stage, the data is pre-processed for the PDR algorithm. A standard coordinate rotation technique is used for converting the given data from the *device coordinate system* (DCS) to the *global coordinate system* (GCS).

[1]We expect the pilgrim to carry a smartphone device with a pre-installed software application. The used smartphone must include a GPS and an IMU to operate the software properly.

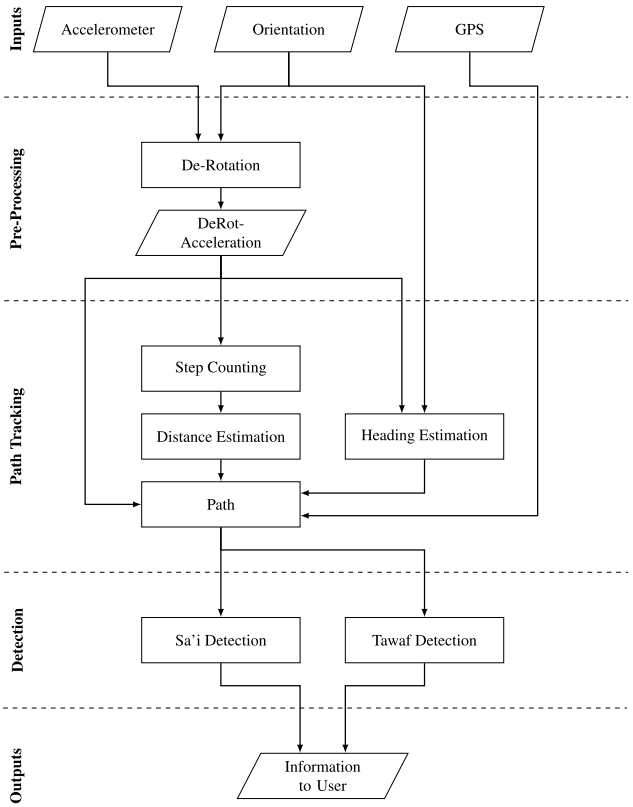

FIGURE 1. Diagram of the proposed ritual detection and monitoring system.

In the second stage, the PDR technique is used to infer the user's path from the pre-processed data by step counting and heading estimation. Step counting, which is mainly inferred from the accelerometer, is used for step detection and stride length estimation. As for heading estimation, it is mainly inferred from the orientation sensor.

The final stage of the proposed framework is to detect the users' activity and provide them with useful information based on their location and situation.

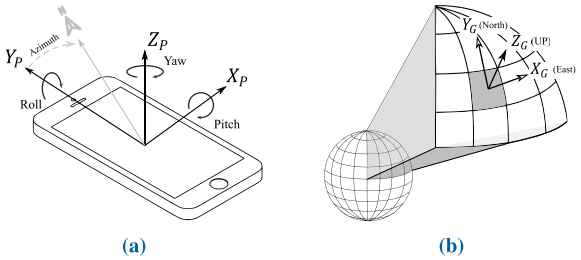

FIGURE 2. (a): Device Coordinate System (DCS) with the three angles visualized. (b): Global Coordinate System (GCS).

A. PRE-PROCESSING

The data provided by smartphone sensors is measured with respect to the smartphone's coordinate system (i.e., DCS).

Since smartphones are held in different positions and orientations with respect to different pilgrims, the fetched smartphone sensor data does not directly indicate the pilgrim's velocity and heading. Rendering the data useful for step counting and heading estimation requires applying a proper rotation matrix to express the raw data in terms of the GCS. Fig. 2 illustrates the difference between the two conventional coordinate systems (i.e., DCS and GCS). The rotation matrix used for conversion between the two systems is given by

$$R(\theta,\phi) = \begin{bmatrix} \cos\phi & 0 & -\sin\phi \\ \sin\theta\sin\phi & \cos\theta & \sin\theta\cos\phi \\ \cos\theta\sin\phi & -\sin\theta & \cos\theta\cos\phi \end{bmatrix} \quad (1)$$

where θ and ϕ denote pitch and roll angles, respectively. It should be noticed that (1) is used for adjusting the tilt of the DCS to be aligned with the xy plane of the GCS. As far as the step counting and heading estimation processes are concerned, only *tilt compensation* [39] for the fetched acceleration vector, $\boldsymbol{a}_{DCS}$, from the device's IMU unit -is required.

Therefore, the corrected acceleration components, $\boldsymbol{a}_{GCS}$, is given by

$$\boldsymbol{a}_{GCS} = R(\theta,\phi)^{\top}\boldsymbol{a}_{DCS} \quad (2)$$

B. PDR FOR PATH TRACKING

For the path tracking task, we opted for the PDR technique due to two main reasons. First, since most of the Umrah rituals are performed in an indoor environment, PDR was chosen as it relies solely on the inertial sensors provided in the smartphone. Furthermore, PDR does not require an external infrastructure to be installed, unlike BLE or Wi-Fi-based methods [19]. PDR technique [24], [25], [26] consists of two main stages. The first stage is step counting and travel distance estimation. The second stage is updating the heading angle after each detected step to infer the corresponding path. Fig. 3 illustrates the process of drawing the user's path using PDR technique. The position of the user at time instant t is given by

$$\begin{aligned} N_t &= N_{t-1} + SL_{t-1} \times \cos\Psi_{t-1} \\ E_t &= E_{t-1} + SL_{t-1} \times \sin\Psi_{t-1} \end{aligned} \quad (3)$$

where N_t and E_t are the current northing and easting, N_{t-1} and E_{t-1} are the previous coordinates, SL_{t-1} is the length of the previous step, and Ψ_{t-1} is the previous heading angle with respect to the north. This section studies the step counting process, and heading estimation.

1) STEP DETECTION

Step counting is the main process in PDR systems [24], along with heading estimation. Rather than abiding by the standard definition of a gait cycle [40], [41], which is convenient for bio-mechanical simulation considerations, we follow the step-phase definition as in [24] which describes the typical behavior of a pedestrian's acceleration.

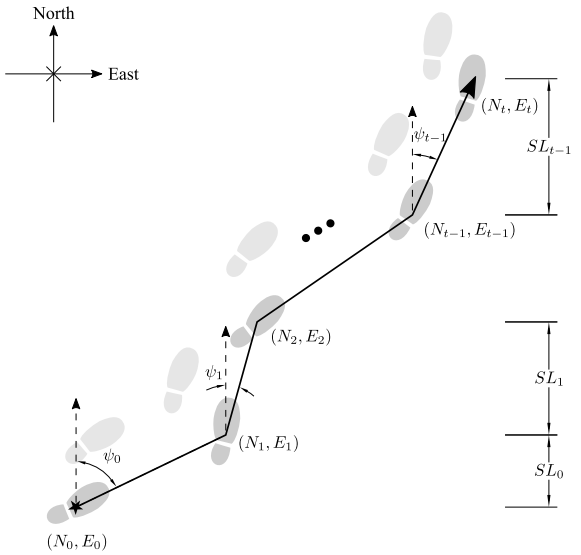

FIGURE 3. Pedestrian dead reckoning (PDR) path illustration.

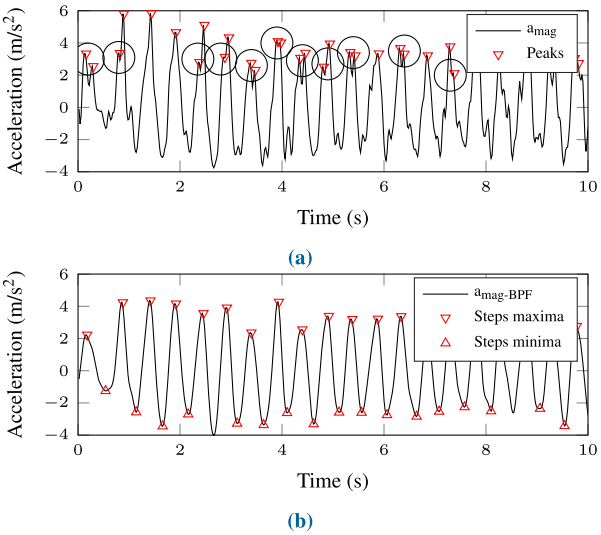

FIGURE 4. Smartphone acceleration during a normal walk shows (a) the double (fake) peaks, and (b) the z-component of acceleration after BPF.

A possible approach for step detection is to monitor the smartphone's acceleration [24], [42]. Regardless of the phone position relative to the user, each step has a significant contribution to the acceleration magnitude, given by

$$a = \sqrt{a_x^2 + a_y^2 + a_z^2} \quad (4)$$

Using this approach for step detection, however, yields erroneous results due to two sources of distortion. First, small-scale fluctuations of the phone while moving, and second, sudden rotations of the user that results in large-scale noise. The first problem results in double (fake) peaks like the ones encircled in Fig. 4a. To solve this problem, a Band

Pass Filter (BPF) with cut-off frequencies of $(0.5 - 10$ Hz) is applied. The cut-off frequencies were obtained empirically to minimize the step counting error. The second problem (i.e., sudden rotations) results in undesirable peaks due to the sudden increments in the global horizontal acceleration components. These noisy peaks cannot be removed with filters as they are identical to the real peaks. Due to this issue, acceleration magnitude obtained from (4) is not always the best option for step counting. However, since this problem results from changes in the global horizontal acceleration components only, the global vertical component of the acceleration can be used for step counting instead of the magnitude. This component can be obtained using the tilt compensation technique discussed in Section II-A. Fig. 4b shows a plot of the isolated vertical acceleration component in time after applying BPF to remove the double peaks.

2) DISTANCE ESTIMATION

The ultimate goal of step counting is to estimate the crossed distance by the user and draw his path, which will be used accordingly in the detection algorithm. In this work, the Weinberg formula given by

$$SL_i = K\sqrt{a_{max,i} - a_{min,i}} \tag{5}$$

is used to estimate the length of each step taken by the user [43], [44]. Weinberg formula is an empirical relation that is commonly utilized in PDR systems to estimate the step length with respect to the user's acceleration.

In (5), SL_i is the length of the i^{th} step that occurred in a certain time window, $a_{max,i}$ and $a_{min,i}$ are the maximum and minimum acceleration values in the same time window, respectively, and K-factor is a constant for unit conversion that is set depending on the user's step size. In our study, we use two different approaches to tune the value of K. The first approach is to train the tuning process based on GPS data. If GPS data is not available, as in an indoor environment, we set the step length to its average (73.6 cm [43]) and train the K-factor so that the resultant average step length matches this value. The sum of step lengths during the desired duration results in the distance crossed by the user, which will be combined with the heading angle (i.e., the last stage of PDR) to draw the user's path.

Although distance estimation is needed for path tracking, accurate estimations are not required for a valid detection of the rituals as will be discussed in II-C. Therefore, even if the step length was chosen to be constant, the algorithm is still functioning. In other words, the output path will have the same shape but will be scaled according to the K-factor and will not affect the detection performance.

3) HEADING ESTIMATION

The orientation sensor is used to update the heading of the user at each step. However, as the smartphone can be randomly carried by the user, a method for correcting the phone orientation to ensure the consistency of the smartphone with the direction of the user is needed.

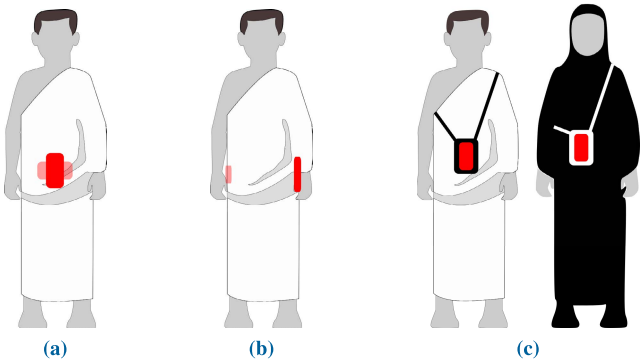

FIGURE 5. Front view of the pilgrim with common phone settings. The phone is positioned horizontally or vertically in a belt fastened on the (a) front side, (b) left or right sides or (c) in a bag held on the front side of the pilgrim.

Albeit random, typical smartphone settings and orientations during Umrah activities can be predicted. Two common settings are depicted in Fig. 5a and 5b. The front bag setting in Fig. 5c is similar to the front belt setting in Fig. 5a in terms of the pilgrim's heading analysis. Ideally, there are two possible phone orientations for every setting in Fig. 5. If the longitudinal side of the phone is perpendicular to the xy-plane of the GCS (See Fig. 2b), then the phone position is vertical. If the longitudinal side of the phone is parallel to the xy-plane of the GCS, then the phone position is horizontal.

Another common setting for the phone is when it is held in front of the user by his hand. We consider two possible phone positions for this setting as well. One position is the portrait mode, which is similar to the vertical position, and the second position is the landscape mode, which is similar to the horizontal position.

Considering these pre-defined positions for the smartphone while performing the rituals and modifying the heading estimation accordingly; will ease the process of the heading correction significantly compared to the random held situation, and hence, reduce the complexity of the model and the real-time processing.

To successfully estimate the pilgrim's heading with respect to his smartphone, it is first required to detect the smartphone orientation using the uncompensated acceleration components. Smartphone orientation is determined by identifying the component dominated by the acceleration of gravity. Compared to the other acceleration components, the target component, a_i, is their maximum. In other words, we seek a_i such that

$$a_i = \max\{|a_x|, |a_y|, |a_z|\} \tag{6}$$

where $\{a_x, a_y, a_z\}$ is a set of the uncompensated components of the fetched vector, $\boldsymbol{a}_{DCS}$. Fig. 6 shows the acceleration for three different cases; vertical, horizontal, and on the hand.

After determining the gravity acceleration component, a_i, tilt compensation is applied to the acceleration vector. Fig. 7b and 7c illustrate the corrected acceleration directions of the phone that correspond to the settings depicted

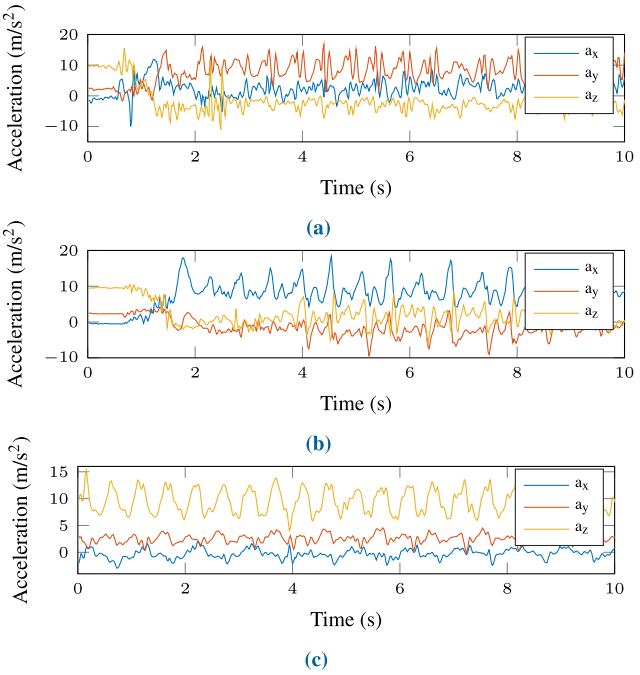

FIGURE 6. Acceleration components for different phone orientations. (a) vertical ($a_i = a_y$), (b) horizontal ($a_i = a_x$), (c) on hand ($a_i = a_z$).

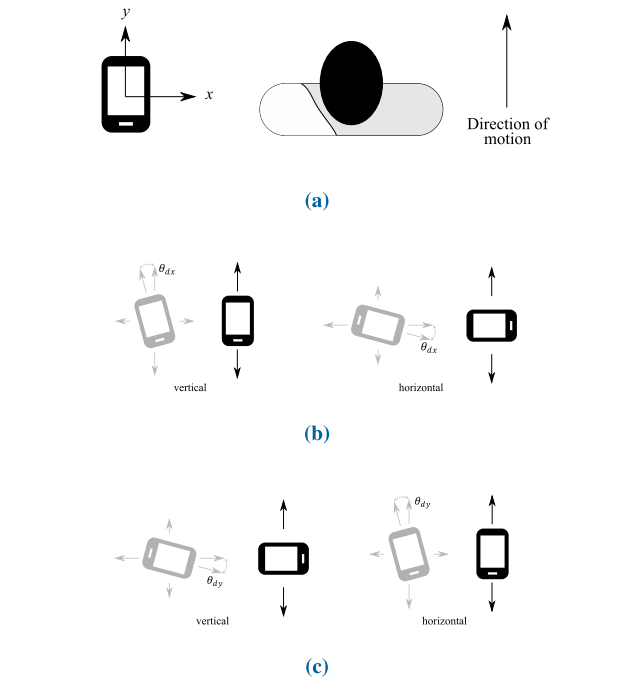

FIGURE 7. (a) Top view of a pilgrim while moving forward. Smartphone heading in (b) front and (c) side positions with respect to the direction of the motion vector after tilt compensation.

in Fig. 5a and 5b, respectively. An angle is assigned to align the heading of the conceivably untilted device with the user's direction of motion as shown in Fig. 7a.

For ideal device orientation (i.e., perfectly vertical or horizontal phone positions), the possible values for the mentioned angle are 0^o, $\pm 90^o$, or -180^o. However, deviation from the ideal situations may cause more than one axis to contribute to the motion vector. Hence, to account for these deviations, we define

$$\theta_{di} = \tan^{-1}\left(\frac{a_i}{\sqrt{a_x^2 + a_y^2}}\right) \tag{7}$$

where θ_{di} is the angle of deviation on a certain axis as illustrated in Fig. 7, a_x and a_y are the corrected acceleration x and y components, respectively, and a_i is the deviated acceleration component obtained by (6).

The angle, θ_{di}, is added to the ideal angle values to correct the heading of the device. The total correction angle for every situation of the device is in Table 1. The acceleration vector, on which the complete heading estimation process operates, is obtained by averaging acceleration values received during the time taken for one step.

In case the smartphone was held in a way that was not identified by the system, the user is notified to adjust his phone in one of the positions as seen in Fig. 5.

TABLE 1. Angle correction for heading estimation.

Position	Orientation	Condition	Angle Correction
On the hand	Portrait mode	-	θ_{dx}
	Landscape mode	$a_x > 0$	$90 + \theta_{dy}$
		$a_x < 0$	$-90 + \theta_{dy}$
Front	Vertical	$a_y > 0$	θ_{dx}
		$a_y < 0$	$-180 + \theta_{dx}$
	Horizontal	$a_x > 0$	$90 + \theta_{dy}$
		$a_x < 0$	$-90 + \theta_{dy}$
Side	Vertical	$a_x < 0$	$-90 + \theta_{dy}$
		$a_x > 0$	$90 + \theta_{dy}$
	Horizontal	$a_y > 0$	θ_{dx}
		$a_y < 0$	$-180 + \theta_{dx}$

C. RITUAL DETECTION

After obtaining the path of the user using the PDR technique, we design algorithms to detect and monitor the activity of the user. In this section, a detailed explanation of the ritual detection algorithms will be provided.

1) TAWAF DETECTION

For the first ritual, Tawaf, an algorithm was built to differentiate between Tawaf performing and non-performing pilgrims. Detecting Tawaf movements allows providing feedback to the user based on their current lap count and position. The algorithm depends mainly on the angle with respect to the Kaaba center for detection. Which is the center of rotation for the Tawaf ritual. The Kaaba center is also used as a reference in our detection as it is a fixed point with known coordinates. Furthermore, several other conditions are used to check for the integrity of the detection to avoid errors as will be shown.

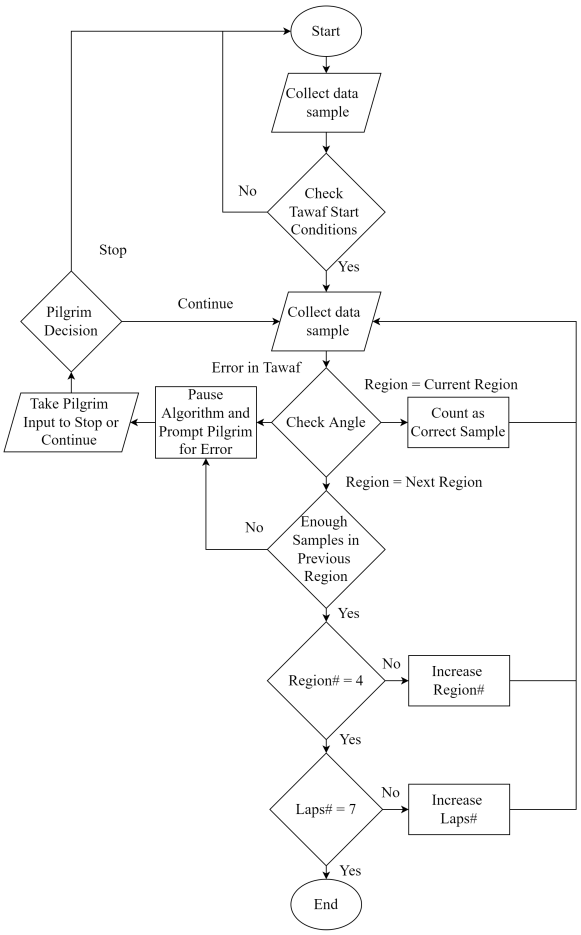

FIGURE 8. Tawaf detection algorithm flowchart.

The inputs to the algorithm are GPS and IMU sensors' data. Fig. 8 shows the overall flowchart for the algorithm. The explanation of the algorithm will focus on the path generated using IMU sensors (the PDR path).

The first step in the algorithm is initializing the path starting point using the GPS. The assumption here is that the GPS data is collected periodically in the background for a certain period to automatically trigger the algorithm. However, if background data collection is disabled, then the activation is needed to start the algorithm. After that, since the center of rotation's location (Kaaba center) has fixed GPS coordinates, the polar coordinates of each point in the path are obtainable with respect to the Kaaba center (center of rotation). The algorithm starts by checking multiple conditions before recognizing that the pilgrim is performing Tawaf, and therefore, triggering the detection algorithm. The main triggering conditions are the distance and the starting angle checks. both check conditions must be fulfilled before triggering the detection. for the distance check, the pilgrim must be within a certain distance from the Kaaba to start the Tawaf. The second one is the starting angle condition, which is fulfilled when the pilgrim is in the correct position around the Kaaba to start the Tawaf. This angle is approximately $-\pi/4$ rads with respect to the north which is the location of Al-Hajar Al-Aswad which is where Muslims start the ritual as indicated by the Tawaf line in Fig. 9).

After that, the algorithm starts monitoring, detecting, and counting the laps. For this part of the algorithm, the Tawaf area is divided into 5 regions, where every region occupies one-quarter of the complete area except for the quarter containing the starting line. This quarter is divided into two in order to create a region barrier at the start/end line of each lap to detect lap endings. This is because completion of the previous region is used as a condition to continue the algorithm. Fig. 9 labels all the mentioned regions.

The algorithm monitors the process by continuously collecting data samples (i.e., pilgrim's position with time). The algorithm ensures that each sample complies with certain conditions to make sure the pilgrim is still performing Tawaf. The main condition involves the angle, through which the algorithm checks if the pilgrim is in the same region as the one indicated by the previous sample. If the pilgrim is not in the current region, the algorithm checks if the pilgrim is in the next/following region. If this is the case, the algorithm checks that the number of samples taken during the previous region is reasonable enough to expect a region transition. This serves as the second condition which is a time restriction where the pilgrim must have spent enough time/samples in the current region for it to be considered a completed region. The third condition is the radius condition, for which the pilgrim must stay within a certain radius or this will cause the algorithm to stop. If any of the conditions to continue the algorithm are broken, then this prompts the pilgrim to check whether they plan to continue, stop, or take a break and then continue the ritual. These actions will go on where the region counter resets every lap, and the algorithm stops when the lap counter reaches 7 (i.e., the pilgrim has finished the Tawaf ritual). To accommodate random errors, a success percentage is introduced as a minimum requirement for the number of samples that need to be correct for proper region transition. The success percentage is currently set to 90%, but it can be adjusted in real-time on-site testing for extreme cases.

2) SA'i DETECTION

After Tawaf, pilgrims move to the Sa'i (Masa'a) area to perform the Sa'i ritual (see Fig. 9). An algorithm is designed to detect the Sa'i and provide useful information to the pilgrim based on his activity. First, the algorithm checks if the pilgrim enters the Masa'a area and starts Sa'i by analyzing the path. Once the pilgrim crosses more than 100 meters, in the direction of *Al-Marwa* (Fig. 9), during which his heading angle is within $[-30^o, 0^o]$ with respect to the North, the Sa'i algorithm is triggered. The direction is obtained directly from the corrected heading angles used to estimate the direction of the pedestrian.

After the automatic trigger is initialized, instantaneous samples are passed through the algorithm to check direction integrity and to calculate the distance traveled through each lap. Practically speaking, pilgrims move in a direction

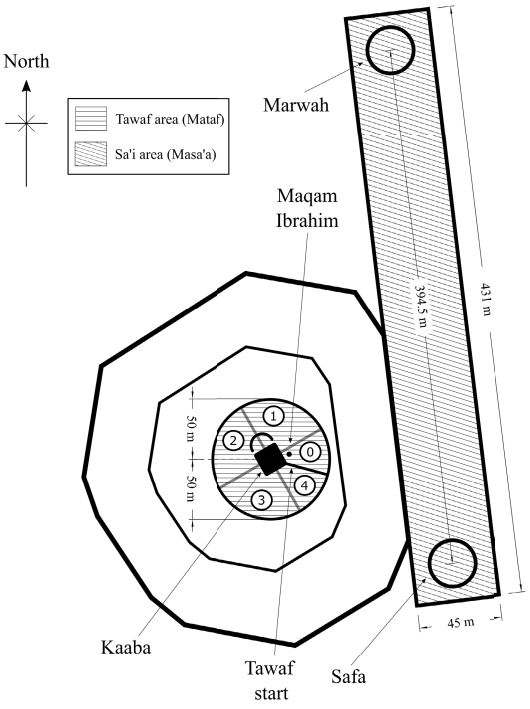

FIGURE 9. Diagram of Tawaf and Sa'i areas. Regions used for detection in the Tawaf Detection Algorithm are shown in the Tawaf area.

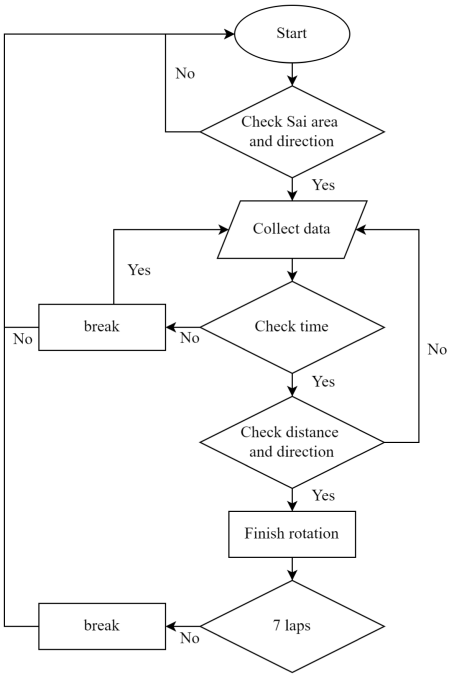

FIGURE 10. Sa'i detection algorithm.

estimated to be within $[-30^o, 0^o]$ during a Safa lap and $[150^o, 180^o]$ during a Marwa lap on average. These values are chosen based on the direction of the Masa'a as shown in Fig. 9. During Sa'i detection, if the pilgrim changed his direction before finishing the lap, or took more than the average time during the lap; a message is sent to him to check if he is continuing or stopping the Sa'i. Once the pilgrim finishes 7 laps, a notification message is sent to the user. An illustration of the developed algorithm is shown in Fig. 10.

III. RESULTS AND DISCUSSION

Detailed results and analysis for path tracking and detection algorithms are reported and discussed in this section.

TABLE 2. Average distance deviation of the path of the inertial sensors with respect to the GPS path.

Trial	Phone position	Distance [m]	Average deviation [m]
1	On hand	205.9	2.89
2	On hand	104.9	1.54
3	On hand	438.5	3.3
4	Front (horizontal)	375.7	7.33
5	Side (horizontal)	403.8	5.6

A. PATH TRACKING

Here we show the results of heading estimation by comparing several paths before and after angle correction. Fig. 11a shows a corrected path in the case of holding the phone by hand. Fig. 11a includes three paths, the GPS path in blue, the PDR path before the angle correction in dotted yellow, and the path using the same technique with angle correction in red. Fig. 11b and Fig. 11c show two paths of the user while carrying the phone horizontally to the belt as in the situation (b).

As discussed in Section II-B, the path detection algorithm monitors the phone position and updates it with each step. Fig. 11d shows the output path in case a transition between different phone positions occurs. First, the user was walking in a straight line while keeping the phone in his pocket, then he/she held it by hand in portrait mode. Fig. 11e shows a simple correction for the heading angle in the case of holding the phone by hand but in a tilted position.

To examine the reliability of the extracted PDR path, we test its accuracy by comparing it with the GPS data as a reference. Table. 2 shows the average distance deviation between the PDR and the GPS paths for different distances and phone positions. Results show that as the distance traveled increases, the deviation between the paths becomes larger due to the accumulation of error. This can be improved by updating the location regularly using GPS. We also notice that the phone position is a major source of error. Unlike holding the phone by hand, putting it in the pocket or holding it to the belt makes it more vulnerable to vibrations, therefore, accuracy reduction is expected even with the proposed heading correction approach.

B. TAWAF DETECTION VALIDATION

To verify the Tawaf detection algorithm, it was tested using a real path as shown in Fig. 12a. The location illustrated in the figure was chosen for its similarity to the Tawaf area. Also,

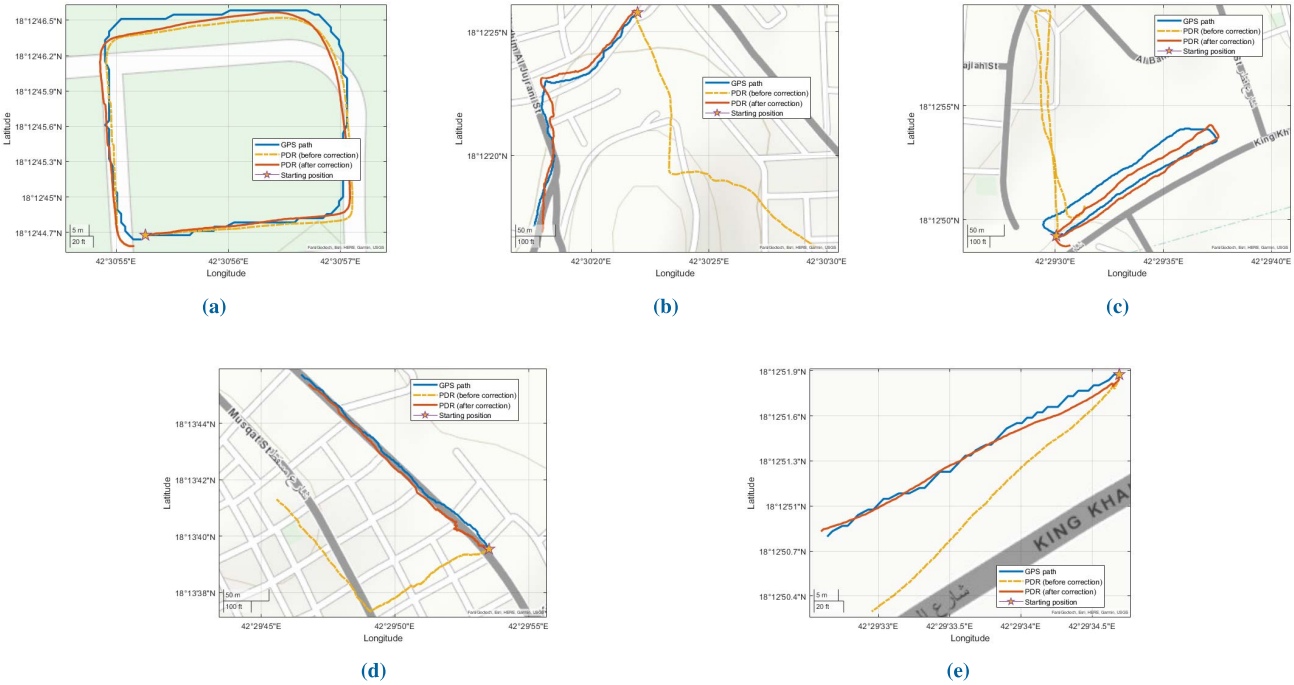

FIGURE 11. PDR paths before and after correction for different situations. (a) phone on the hand (portrait mode), (b) and (c) phone carried horizontally to the belt, in (d) phone was initially in the pocket then carried by hand, and (e) phone on the hand (tilted).

this location is an open area where GPS data is reliable and can be used as a benchmark for path extraction and Tawaf detection. Fig. 12b shows the resulting PDR and the GPS paths. The similarity between the two extracted paths proves the reliability of the implemented PDR in terms of Tawaf detection. It can be noticed, however, that some walking patterns in the PDR path appear to be out of sync compared to the GPS path in Fig. 12b. This means that some path curves are shown in different places on the two paths. Such errors occur due to the difference in sampling rates and the error accumulation in the PDR path when using the inertial sensors as compared to the GPS. The smartphone used in the experiment has a fixed sampling rate of 1 Hz for GPS data, compared to 50 Hz for the inertial sensors. Naturally, these errors propagate through PDR, which is an iterative process. Error propagation does not occur in GPS as it uses an absolute reference.

Despite the apparent mismatch between the fetched paths at various points in 12b, the overall similarity enables an accurate Tawaf detection. To validate Tawaf detection, PDR and GPS paths are inputted individually to the detection algorithm. Fig. 14 shows the final output of the algorithm. In both cases, Tawaf was detected correctly, including the start/end points, regions, and number of laps. Each lap was detected individually and at the correct time. This shows that both the path extraction and the Tawaf detection work properly in the correct conditions. The path was started after the starting Tawaf position, this is to test that the start position conditions are working. This means that the first lap (Orange) will not be counted as a part of Tawaf which is why it is shown as the pre-Tawaf path in the figures below. This also confirms that if a pilgrim did not start Tawaf at the correct starting angle range, the first lap will not count because it was not complete. The path in the test was completed at the end with 7 complete laps to confirm a complete Tawaf detection. This link[2] shows a video demonstrating the algorithm running and detecting the ritual from the path. The PDR path is also very smooth compared to the path from the GPS. This is again due to the high sampling rate used in the IMU sensors which is not possible for the GPS sensor. The algorithm also handles any errors that break the Tawaf continuity conditions (e.g. going in the reverse direction) by pausing the process and waiting for the pilgrim's response. If the response is to continue the data collection will continue from the last correct sample. If there is no response, or the response was to stop the algorithm, then the algorithm will reset.

Although results for Tawaf detection are satisfactory in the experiment conditions, further testing is needed to see the performance in real Tawaf conditions. This is due to many factors such as the different geographical locations and the large number of mobile phones in the area which could affect the GPS data. Also, the two methods (GPS and PDR) need to be tested independently to study their effect on the battery life. Notably, the PDR curve is very smooth compared to the GPS curve due to its high sampling. However, as both paths were successfully detected, it might be worth lowering the

[2]Algorithm Demonstration Video: youtu.be/O3bFb-4c4kE

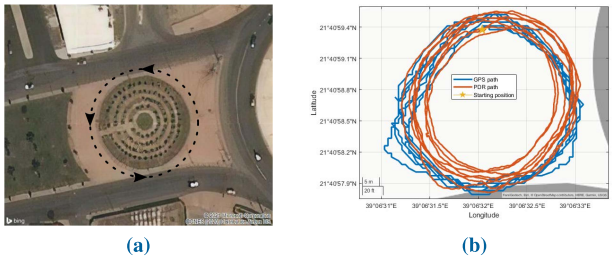

(a) (b)

FIGURE 12. (a) Tawaf test verification area, and (b) Extracted paths used for verification.

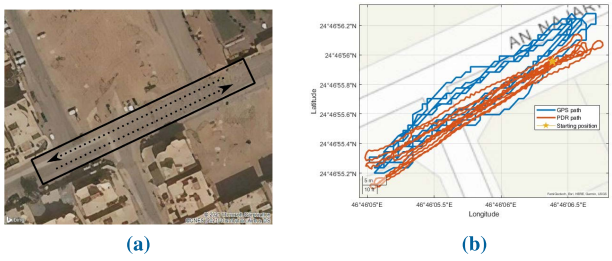

(a) (b)

FIGURE 13. (a) Sa'i test verification area, and (b) Extracted paths used for verification.

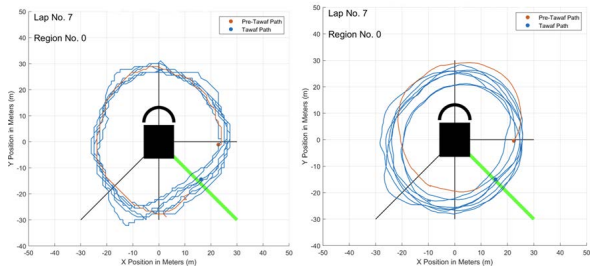

(a) (b)

FIGURE 14. Tawaf detection algorithm output visualization (a) with real data using GPS, and (b) inertial sensors (PDR).

sampling of the IMU sensors to optimize energy consumption. Although the error accumulation could cause an error the longer the path, it can be addressed by re-initializing the path periodically using the GPS to reset the accumulated error.

C. SA'I DETECTION VALIDATION

Unlike Tawaf, GPS is not expected to perform well in terms of path tracking for pilgrims performing Sa'i, which is an indoor environment. Therefore, to validate the Sa'i detection algorithm, an experiment is conducted in an open area as seen in Fig. 13a to simulate Sa'i and compare the PDR path with the GPS path. Like Tawaf detection validation, the PDR path was extracted and compared to the GPS path. The two paths are shown in Fig. 13b, where the PDR path is plotted in red and the GPS path is plotted in blue.

As illustrated in Fig. 10, the algorithm considers time, distance, and heading direction to count the lap. Therefore, unless the user starts from the correct starting point of the Sa'i ritual, labeled as Safa in Fig. 9, the algorithm will not be triggered, and laps will not be counted. On the other hand, when a user performs extra laps (i.e., more than seven laps), which is the case in Fig. 13b, the algorithm terminates the activity and sends a message that the Sa'i ritual is completed.

Considering the similarity between the two paths in Fig. 13b, the PDR-based tracking approach is successful. It can be noticed that there are also some synchronization issues due to, as discussed in III-B, the difference in sampling rates between GPS and the IMU unit. It can be noticed that the PDR path is smoother than the GPS path due to the high sampling rate for the IMU unit.

IV. LIMITATIONS

One major limitation to the process explained in II-C is the need for periodically collecting background GPS data before triggering the detection algorithm. The sampling rate of GPS is required to be high enough to detect the start of the ritual. Otherwise, the algorithm may not be triggered and, consequently, may not be able to perform its task correctly. Background collection of the GPS data could affect the battery life of the phone, especially at high sampling rates. More analysis is needed to determine the optimal period of background GPS data collection to automatically detect the starting point of the ritual and minimize battery utilization. Also, if background data collection is disabled, the detection process will require user activation.

Another limitation is imposed by the algorithm's dependency on specific phone positions. Phone positions that are not considered in II-B3 may occur, albeit rarely, due to unexpected situations like falling and sliding. The algorithm handles such abnormalities by requesting the user to adjust their device, which can be inconvenient for the user. Another situation where user's input is required is when they decide to take a break. If the algorithm is not informed directly by the user that Tawaf or Sa'i is stopped, the algorithm stops tracking and then restarts at the beginning of the next lap. In this case, the detection process will be incomplete, since the pilgrim needs to complete the current lap when they return to the ritual. Therefore, a better error handling process that enables the algorithm to automatically recover when the pilgrim returns to the correct path would be beneficial in the future.

Finally, the proposed algorithm naturally inherits the limitations of the employed tracking algorithm. The main drawback of PDR is error accumulation in its extracted path points (see Section III-A). As a solution, the use of GPS data to correct the paths regularly is proposed. However, GPS access is not always available during the rituals, hence, the system is more vulnerable to making errors in indoor areas like the Sa'i area.

V. CONCLUSION

In this research, an algorithm is designed to track pilgrims who are performing Umrah and detect their activities. The path detection algorithm utilizes IMU sensors to estimate

the change in the pilgrim's position and heading, and then update his location. Several conditions were used in detection algorithms to assist the output decision regarding the situation and the activity of the user. The designed system provides the pilgrim with useful information, depending on his activity and location, such as the number of laps, real-time guidance, and supplications. Deviation from the path due to accumulation of error is investigated for different phone positions. The deviated path can be restored by the assessment of GPS.

In future research, more work is needed to apply and test both the path tracking and ritual detection in real-world conditions to improve the overall system and especially the Sa'i detection algorithm. An introduction of a better error handling system might prove highly beneficial as people may not have the time to look at their phones during these rituals. It is also important to look at the optimization of the parameters used in the algorithms such as the sampling rates of inertial sensors and GPS background data collection frequency. Furthermore, the continuation of this research might prove useful in the area of crowd management as the number of people who perform such rituals all year round is huge, especially during the Hajj season.

REFERENCES

[1] (2019). *Umrah Statistics Bulletin*. Accessed: Jul. 2020. [Online]. Available: https://www.stats.gov.sa/en/6590-0

[2] A. A. Owaidah, D. Olaru, M. Bennamoun, F. Sohel, and R. N. Khan, "Modelling mass crowd using discrete event simulation: A case study of integrated Tawaf and Sayee rituals during Hajj," *IEEE Access*, vol. 9, pp. 79424–79448, 2021.

[3] E. A. Khan and M. K. Y. Shambour, "An analytical study of mobile applications for Hajj and Umrah services," *Appl. Comput. Informat.*, vol. 14, no. 1, pp. 37–47, Jan. 2018.

[4] E. J. Lind, S. Jayaraman, S. Park, R. Rajamanickam, R. Eisler, G. Burghart, and T. McKee, "A sensate liner for biomedical monitoring applications," *Stud. Health Technol. Informat.*, vol. 50, no. 4, pp. 258–264, 1998.

[5] J. Farringdon, A. J. Moore, N. Tilbury, J. Church, and P. D. Biemond, "Wearable sensor badge & sensor jacket for context awareness," in *Proc. 3rd Int. Symp. Wearable Comput.*, Oct. 1999, pp. 107–113.

[6] C. A. Ronao and S.-B. Cho, "Deep convolutional neural networks for human activity recognition with smartphone sensors," in *Proc. Int. Conf. Neural Inf. Process.* Cham, Switzerland: Springer, 2015, pp. 46–53.

[7] C. A. Ronao and S.-B. Cho, "Human activity recognition with smartphone sensors using deep learning neural networks," *Expert Syst. Appl.*, vol. 59, pp. 235–244, Oct. 2016.

[8] A. Bayat, M. Pomplun, and D. A. Tran, "A study on human activity recognition using accelerometer data from smartphones," *Proc. Comput. Sci.*, vol. 34, pp. 450–457, Jan. 2014. [Online]. Available: https://www.sciencedirect.com/science/article/pii/S1877050914008643

[9] I. Andrey, "Real-time human activity recognition from accelerometer data using convolutional neural networks," *Appl. Soft Comput.*, vol. 62, pp. 915–922, Jan. 2017. [Online]. Available: https://www.sciencedirect.com/science/article/pii/S1568494617305665

[10] T. Choudhury, S. Consolvo, B. Harrison, J. Hightower, A. LaMarca, L. LeGrand, A. Rahimi, A. Rea, G. Bordello, B. Hemingway, P. Klasnja, K. Koscher, J. Landay, J. Lester, D. Wyatt, and D. Haehnel, "The mobile sensing platform: An embedded activity recognition system," *IEEE Pervasive Comput.*, vol. 7, no. 2, pp. 32–41, Apr./Jun. 2008.

[11] J. A. Ward, P. Lukowicz, G. Troster, and T. E. Starner, "Activity recognition of assembly tasks using body-worn microphones and accelerometers," *IEEE Trans. Pattern Anal. Mach. Intell.*, vol. 28, no. 10, pp. 1553–1567, Oct. 2006.

[12] G. Laput, K. Ahuja, M. Goel, and C. Harrison, "Ubicoustics: Plug-and-play acoustic activity recognition," in *Proc. 31st Annu. ACM Symp. User Interface Softw. Technol.*, 2018, pp. 213–224.

[13] P. Turaga, R. Chellappa, V. S. Subrahmanian, and O. Udrea, "Machine recognition of human activities: A survey," *IEEE Trans. Circuits Syst. Video Technol.*, vol. 18, no. 11, pp. 1473–1488, Nov. 2008.

[14] A. M. Khan, "Recognizing physical activities using the axivity device," in *Proc. 5th Int. Conf. eHealth, Telemed., Social Med. (eTELEMED)*, Mar. 2013, pp. 4–7. [Online]. Available: http://www.comnets.uni-bremen.de/cewit-tzi-workshop-2013/PDF/papers/Khan.pdf

[15] X. Su, H. Tong, and P. Ji, "Activity recognition with smartphone sensors," *Tsinghua Sci. Technol.*, vol. 19, no. 3, pp. 235–249, Jun. 2014.

[16] Z. Chen, S. Xiang, J. Ding, and X. Li, "Smartphone sensor-based human activity recognition using feature fusion and maximum full a posteriori," *IEEE Trans. Instrum. Meas.*, vol. 69, no. 7, pp. 3992–4001, Jul. 2020.

[17] *Tawaf App*. Accessed: Mar. 11, 2021. [Online]. Available: http://www.gistic.org/tawafapp/

[18] General Presidency of the Affairs of the Grand Mosque and the Prophet's Mosque. (Jan. 2019). *Al Maqsad*. [Online]. Available: https://apps.apple.com/sa/app/al-maqsad/id1447123573

[19] I. Ashraf, S. Hur, and Y. Park, "Smartphone sensor based indoor positioning: Current status, opportunities, and future challenges," *Electron.*, vol. 9, no. 6, p. 891, 2020. [Online]. Available: https://www.mdpi.com/2079-9292/9/6/891

[20] N. Yu, Y. Li, X. Ma, Y. Wu, and R. Feng, "Comparison of pedestrian tracking methods based on foot-and waist-mounted inertial sensors and handheld smartphones," *IEEE Sensors J.*, vol. 19, no. 18, pp. 8160–8173, Sep. 2019.

[21] I. Khan, S. Khusro, S. Ali, and J. Ahmad, "Sensors are power hungry: An investigation of smartphone sensors impact on battery power from lifelogging perspective," *Bahria Univ. J. ICT*, vol. 9, pp. 8–19, Dec. 2016.

[22] W. Xu, L. Liu, S. Zlatanova, W. Penard, and Q. Xiong, "A pedestrian tracking algorithm using grid-based indoor model," *Autom. Construct.*, vol. 92, pp. 173–187, Aug. 2018.

[23] D. Titterton, J. L. Weston, and J. Weston, *Strapdown Inertial Navigation Technology*, vol. 17. Edison, NJ, USA: IET, 2004.

[24] N.-H. Ho, P. H. Truong, and G.-M. Jeong, "Step-detection and adaptive step-length estimation for pedestrian dead-reckoning at various walking speeds using a smartphone," *Sensors*, vol. 16, no. 9, p. 1423, 2016.

[25] M. Khedr and N. El-Sheimy, "S-PDR: SBAUPT-based pedestrian dead reckoning algorithm for free-moving handheld devices," *Geomatics*, vol. 1, no. 2, pp. 148–176, Mar. 2021. [Online]. Available: https://www.mdpi.com/2673-7418/1/2/10

[26] J. Geng, L. Xia, J. Xia, Q. Li, H. Zhu, and Y. Cai, "Smartphone-based pedestrian dead reckoning for 3D indoor positioning," *Sensors*, vol. 21, no. 24, p. 8180, 2021. [Online]. Available: https://www.mdpi.com/1424-8220/21/24/8180

[27] M. Khedr and N. El-Sheimy, "S-pdr: Sbaupt-based pedestrian dead reckoning algorithm for free-moving handheld devices," *Geomatics*, vol. 1, no. 2, pp. 148–176, 2021. [Online]. Available: https://www.mdpi.com/2673-7418/1/2/10

[28] A. Brajdic and R. Harle, "Walk detection and step counting on unconstrained smartphones," in *Proc. ACM Int. joint Conf. Pervasive ubiquitous Comput.*, 2013, pp. 225–234.

[29] F. Gu, K. Khoshelham, J. Shang, F. Yu, and Z. Wei, "Robust and accurate smartphone-based step counting for indoor localization," *IEEE Sensors J.*, vol. 17, no. 11, pp. 3453–3460, Jun. 2017.

[30] G. Rodríguez, F. Casado, R. Iglesias, C. Regueiro, and A. Nieto, "Robust step counting for inertial navigation with mobile phones," *Sensors*, vol. 18, no. 9, p. 3157, Sep. 2018.

[31] V. T. Pham, D. A. Nguyen, N. D. Dang, H. H. Pham, V. A. Tran, K. Sandrasegaran, and D.-T. Tran, "Highly accurate step counting at various walking states using low-cost inertial measurement unit support indoor positioning system," *Sensors*, vol. 18, no. 10, p. 3186, 2018.

[32] A. C. Dirican and S. Aksoy, "Step counting using smartphone accelerometer and fast Fourier transform," *Sigma J. Eng. Nat. Sci.*, vol. 8, pp. 175–182, Oct. 2017.

[33] X. Kang, B. Huang, and G. Qi, "A novel walking detection and step counting algorithm using unconstrained smartphones," *Sensors*, vol. 18, no. 1, p. 297, 2018.

[34] A. Poulose, B. Senouci, and D. S. Han, "Performance analysis of sensor fusion techniques for heading estimation using smartphone sensors," *IEEE Sensors J.*, vol. 19, no. 24, pp. 12369–12380, Dec. 2019.

[35] X. Yuan, S. Yu, S. Zhang, G. Wang, and S. Liu, "Quaternion-based unscented Kalman filter for accurate indoor heading estimation using wearable multi-sensor system," *Sensors*, vol. 15, no. 5, pp. 10872–10890, May 2015.

[36] V. Thio, K. B. Ånonsen, and J. K. Bekkeng, "Relative heading estimation for pedestrians based on the gravity vector," *IEEE Sensors J.*, vol. 21, no. 6, pp. 8218–8225, 2021.
[37] *Position Sensors: Android Developers*. Accessed: Apr. 20, 2021. [Online]. Available: https://developer.android.com/guide/topics/sensors/sensors_position
[38] A. Abadleh, B. M. Al-Mahadeen, R. M. AlNaimat, and O. Lasassmeh, "Noise segmentation for step detection and distance estimation using smartphone sensor data," *Wireless Netw.*, vol. 27, no. 4, pp. 2337–2346, 2021.
[39] V. Grygorenko, "Sensing—Magnetic compass with tilt compensation," Cypress, San Jose, CA, USA, Tech. Rep. AN2272, 2011.
[40] A. Alamdari and V. Krovi, "Chapter two—A review of computational musculoskeletal analysis of human lower extremities," in *Human Modelling for Bio-Inspired Robotics*, J. Ueda and Y. Kurita, Eds. New York, NY, USA: Academic, 2017, pp. 37–73. [Online]. Available: https://www.sciencedirect.com/science/article/pii/B9780128031377000033
[41] L. M. Silva and N. Stergiou, "The basics of gait analysis," in *Biomechanics and Gait Analysis*, N. Stergiou, Ed. New York, NY, USA: Academic, 2020, pp. 225–250. [Online]. Available: https://www.sciencedirect.com/science/article/pii/B9780128133729000075
[42] W. Lu, F. Wu, H. Zhu, and Y. Zhang, "A step length estimation model of coefficient self-determined based on peak-valley detection," *J. Sensors*, vol. 2020, pp. 1–14, Nov. 2020.
[43] A. Spinillo, A. Bernuzzi, C. Cevini, R. Gulminetti, S. Luzi, A. Santolo, O. P. Jasuja, S. Harbhajan, and K. Anupama, "Estimation of stature from stride length while walking fast," *Forensic Sci. Int.*, vol. 86, pp. 181–186, May 1997.
[44] M. Vezocnik, R. Kamnik, and M. B. Juric, "Inertial sensor-based step length estimation model by means of principal component analysis," *Sensors*, vol. 21, no. 10, p. 3527, 2021. [Online]. Available: https://www.mdpi.com/1424-8220/21/10/3527

KHALIL CHIKHAOUI received the B.Sc. degree in electrical engineering from the King Fahd University of Petroleum and Minerals (KFUPM), Dhahran, Saudi Arabia, in 2021, where he is currently pursuing the master's degree in electrical engineering. His research interests include image processing, computer vision, machine learning, and deep learning.

MOHAMMED ELRASHIDY received the B.Sc. degree in electrical engineering from KFUPM, in 2021, where he is currently pursuing the M.Sc. degree with the Electrical Engineering Department. His research interests include graph signal processing, adaptive filtering, and deep learning. His current research is focusing on simultaneous information and power transmission in wireless networks.

MOTAZ ALFARRAJ (Member, IEEE) received the B.Sc. degree in electrical engineering from KFUPM, in 2013, and the M.Sc. and Ph.D. degrees in electrical and computer engineering from the Georgia Institute of Technology, Atlanta, GA, USA, in 2016 and 2019, respectively. He is currently an Assistant Professor with the Electrical Engineering Department, KFUPM. He is also the Director of the SDAIA-KFUPM Joint Research Center for Artificial Intelligence (JRC-AI). His research interests include machine learning, deep learning, computer vision, and image processing. His research focuses on the integration of physics in data-driven systems to enable effective learning from noisy data for applications in oil and gas exploration and production. He is a member of Society of Exploration Geophysicists (SEG), and Society of Petroleum Engineers (SPE).

ALI H. MUQAIBEL (Senior Member, IEEE) received the B.Sc. and M.Sc. degrees from the King Fahd University of Petroleum and Minerals (KFUPM), Dhahran, Saudi Arabia, in 1996 and 1999, respectively, and the dual Ph.D. degree from the Virginia Polytechnic Institute and State University, Blacksburg, VA, USA, in 2003. During his study with Virginia Tech, he was with the Time Domain and RF Measurements Laboratory and the Mobile and Portable Radio Research Group. He was a Visiting Associate Professor with the Center of Advanced Communications, Villanova University, Villanova, PA, USA, in 2013, a Visiting Professor with the Georgia Institute of Technology, Atlanta, GA, USA, in 2015, and a Visiting Scholar with the King Abdullah University for Science and Technology, Thuwal, Saudi Arabia, from 2018 to 2019. He is currently a Professor with the Electrical Engineering Department, KFUPM. He is also the Director of the Center for Communication Systems and Sensing. He has authored two book chapters and more than 130 articles. His research interests include direction of arrival estimation, throughwall-imaging, localization, channel characterization, and ultra-wideband signal processing. He was a recipient of many awards in the excellence in teaching, advising, and instructional technology.

RIDA SADAGAH received the B.Sc. degree in electrical engineering from the King Fahd University of Petroleum and Minerals (KFUPM), Dhahran, Saudi Arabia, and the Graduate degree (Hons.) in communications systems. He is currently working as an Automation & Control Systems Engineer at Saudi Aramco. His research interests include wireless communications, machine learning, and image processing.

ABDULLAH SHARQAWI received the B.Sc. degree in electrical engineering from the King Fahd University of Petroleum and Minerals (KFUPM), Dhahran, KSA, in 2021. Also, he has a concentration in communication systems with KFUPM. His research interests include networks, fiber-optic communication, wireless communication, and machine learning.